

The Tungsten Project: Dielectronic Recombination Data For Collisional-Radiative Modelling In ITER

S. P. Preval^{1,a)}, N. R. Badnell¹ and M. G. O’Mullane¹

¹*Department of Physics, University of Strathclyde, Glasgow, G4 0NG, United Kingdom*

^{a)}Corresponding author: simon.preval@strath.ac.uk

Abstract. Tungsten is an important metal in nuclear fusion reactors. It will be used in the divertor component of ITER (Latin for ‘the way’). *The Tungsten Project* aims to calculate partial and total DR rate coefficients for the isonuclear sequence of Tungsten. The calculated data will be made available as and when they are produced via the open access database OPEN- ADAS in the standard *adf09* and *adf48* file formats. We present our progress thus far, detailing calculational methods, and showing comparisons with other available data. We conclude with plans for the future.

INTRODUCTION

Tungsten has been chosen as the plasma facing material that will compose the divertor in the upcoming experimental fusion reaction ITER. The reasons for this are threefold; tungsten has a high melting point, it is resistant to absorption of tritium, and is also able to withstand with large power loads. In preparation for ITER, the Joint European Torus (JET) has been fitted with a beryllium wall and tungsten divertor (Matthews *et al.* [1]). This experimental setup is referred to as the ITER-like wall (ILW). Recent experiments with the ILW have shown reduced absorption of tritium as expected, but they have also shown that this configuration reduces the pedestal temperature in the tokamak from $\sim 1\text{keV}$ to $\sim 700\text{eV}$ (Romanelli and Contributors [2]).

Being a plasma-facing component, tungsten will be sputtered into the divertor plasma, and will make its way into the main body plasma. This can potentially cool the plasma, leading to disruption and quenching. In order to understand the effect this impurity has on the plasma, detailed collisional-radiative (CR) modelling is required. The major caveat to this, however, is the provision of detailed, partial and total dielectronic recombination (DR) rate coefficient data.

This requirement has spurred multiple efforts to calculate such data. Chung *et al.* [3] calculated DR rate coefficient data for the isonuclear sequence of tungsten using FLYCHK, which uses the average-atom method (Zhao and Li [4]). Pütterich *et al.* [5] used ADPAK (Post *et al.* [6, 7]), which is based on the average-atom method also. In order to improve agreement with observation, the authors scaled the ADPAK rates for certain W stages. Finally, Foster [8] covered the isonuclear sequence using the Burgess General Formula (Burgess [9]). In both the Pütterich *et al* and Foster isonuclear data, radiative recombination data was calculated using scaled hydrogenic values. In Figure 1 we have plotted the steady state ionization balance for tungsten using ionization rate coefficients from Loch *et al.* [10], and the recombination rate coefficients of Pütterich and Foster. It can be seen that large discrepancies exist for both the peak abundance temperatures, and the individual ionization fractions.

In addition to isonuclear sequence work, several groups have also calculated detailed DR rate coefficients for individual ions. While not a complete list, a few examples are that of Wu *et al.* [11], who use the Flexible Atomic Code (Gu [12]) to calculate level-resolved DR rate coefficients for $W^{37+} - W^{46+}$, Kwon and Lee [13] who used HULLAC (Bar-Shalom, Klapisch, and Oreg [14]) to calculate W^{45+} , and Peleg *et al.* [15] who also used HULLAC to calculate W^{56+} . Again using HULLAC, Safronova, Safronova, and Beiersdorfer [16], and Behar, Mandelbaum, and Schwob [17] considered DR of W^{63+} . In addition, Preval, Badnell, and O’Mullane [18] have used the AUTOSTRUCTURE code (Badnell [19, 20, 21]) to calculate DR rate coefficients for $W^{56+} - W^{73+}$. AUTOSTRUCTURE has been experimentally verified in previous works such as Savin *et al.* [22].

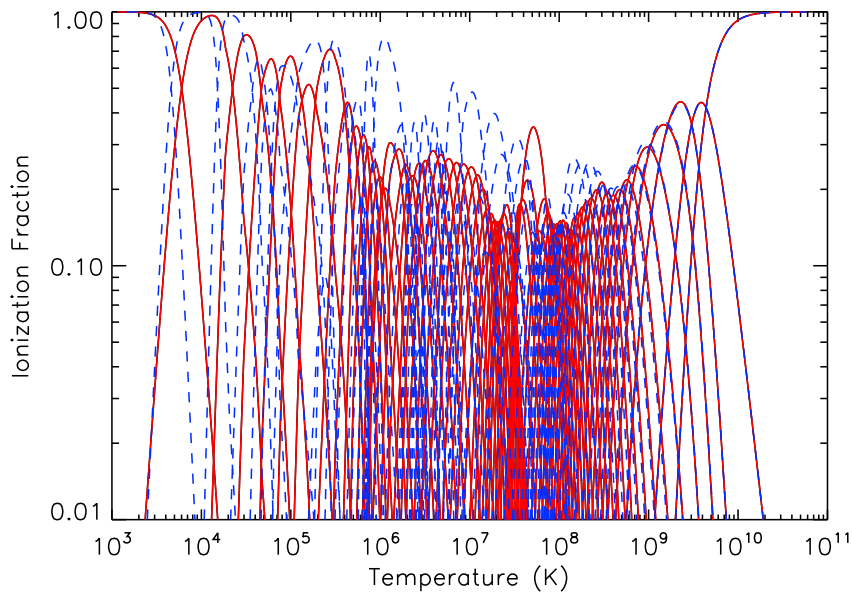


FIGURE 1. Comparison of ionization balances calculated using the recombination rate coefficients of Pütterich *et al.* [5] (red solid curve) and Foster [8] (blue dashed curve). Both curves use the ionization rate coefficients of Loch *et al.* [10].

As final-state-resolved partial DR rate coefficient data is only available for a handful of ions, we have launched *The Tungsten Project*. The project will aim to calculate DR rate coefficients to as high an accuracy as possible for the entire isonuclear sequence of tungsten. In these proceedings, we will describe *The Tungsten Project*, detailing calculational methods, and the data that will be generated. We conclude with a few remarks and the future work we plan to do.

The Tungsten Project - Calculations

As a technical point, different ionisation stages of tungsten will be referred to by the number of valence electrons present in said ion. For example, H-like (one electron) becomes 01-like, and Si-like (14 electrons) becomes 14-like. A detailed description of the calculational method can be found in Preval, Badnell, and O’Mullane [18], however, we provide a brief summary here. All calculations were carried out using the distorted wave code `AUTOSTRUCTURE` (Badnell [19, 20, 21]). `AUTOSTRUCTURE` is able to calculate energy levels, oscillator strengths, photoionization cross sections, and many other quantities. These quantities can be calculated with level resolution (intermediate coupling IC), term resolution (LS coupling), or configuration resolution (configuration average CA) using semi-relativistic kappa-averaged wavefunctions. We label our DR rate coefficient calculations for each ion by the core excitation considered, which is described by the initial and final n of the DR process (n_i and n_f respectively). As an example, a core excitation with $n_i = 3$ and $n_f = 4$ is labeled as 3–4. To decide which core excitations should be calculated in IC for a particular ion, we first calculate them in CA and compare their contribution to the overall total. If it exceeds 5%, we perform the calculation in IC. In addition to calculating DR rate coefficients, we also calculate radiative recombination (RR) rate coefficients, which are important for 00-like to 18-like. In Figure 2 we give an example of calculated IC DR/RR rate coefficients for 15-like tungsten. The figure also shows the cumulative fraction, which shows the relative contribution of each core excitation and the RR rate coefficient to the total recombination rate coefficient. The largest contribution is given first, followed by the largest plus the second largest, and so on.

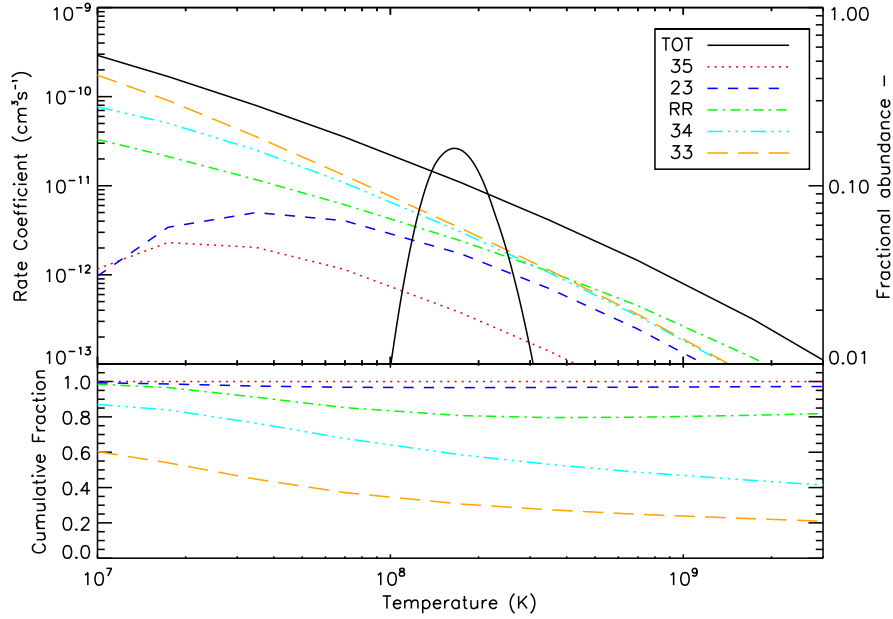


FIGURE 2. Plot of total DR and RR rate coefficients for 15-like W. The fractional abundance for 15-like is also shown (solid black parabola), which is calculated using the recombination data of Pütterich *et al.* [5], and the ionisation rate coefficients of Loch *et al.* [10]. The bottom plot shows the cumulative fraction for each core excitation to the total recombination rate coefficient.

DR

The Rydberg electron DR is calculated for each explicit principal quantum number n up to $n = 25$, after which it is then calculated for n on a logarithmic scale up to $n = 999$. Interpolation is then used to calculate DR for intermediate values of n . Angular momenta ℓ for each n are calculated up to a maximum value such that the DR rate coefficients are numerically converged to $< 1\%$ over the entire ADAS temperature range $z^2(10 - 10^7)\text{K}$, where z is the residual charge. For n values greater than $(\frac{1}{4}\ell^2 + 15)$ AUTOSTRUCTURE approximates a bound wavefunction $P_{n\ell}$ by a zero energy continuum wavefunction $F_{k\ell}(r)$ using the result (Badnell and Pindzola [23])

$$\lim_{n \rightarrow \infty} \left(\frac{\pi v_{n\ell}^3}{2z^2} \right)^{\frac{1}{2}} P_{n\ell}(r) = F_{k\ell}(r)|_{k=0}, \quad (1)$$

where $k^2 = E$, $v_{n\ell} = n - \mu_\ell$, and μ_ℓ is the quantum defect. This approach allows the Hamiltonian to be diagonalized for all n and to allow for the opening up of new Auger channels at high n .

The configurations for the N-electron target consist of all single excitations from each subshell. The N+1 configurations are simply the N-electron configurations with an additional electron. In Table 1 we include an example of the configurations used for 15-like 3–3. Mixing configurations are also included by way of the “one up-one down” rule, as these configurations are typically close to each other in terms of energy, and hence mix strongly.

RR

As with DR, the Rydberg electron RR is calculated for each n up to $n = 25$, and then logarithmically up to $n = 999$. ℓ are included relativistically up to $\ell = 10$, after which a non-relativistic top-up up to $\ell = 150$ is added. This is sufficient to converge bare-like RR to $< 1\%$ over the ADAS temperature range as given above. The N-electron configurations used for RR calculations resemble that of the $\Delta n = 0$ core excitations for DR. All possible excitations of the outermost electron are included plus mixing. Again, the N+1 configurations are just the N-electron configurations plus an electron. The RR rate coefficients include multipolar radiation contributions up to E40 and M39.

TABLE 1. List of configurations included in IC calculation for 15-like 3–3. The left column gives the N-electron configurations, whilst the right gives the N+1-electron configurations. Configurations marked with * are included as mixing configurations.

N-electron	N+1-electron
$3s^23p^3$	$3s^23p^4$
$3s^23p^23d$	$3s^23p^33d$
$3s3p^4$	$3s^23p^23d^2$
$3s3p^33d$	$3s3p^5$
* $3p^5$	$3s3p^43d$
* $3s^23p3d^2$	$3s3p^33d^2$
	* $3p^6$
	* $3p^53d$
	* $3s^23p3d^3$

Comparisons

Ionization Balance

In Figure 3 we compare the ionization balance calculated using the Foster [8] recombination data, and our present calculations. Both recombination data sets use the ionization rate coefficients of Loch *et al.* [10]. For our ionization balance, we include data up to 18-like, after which we use Pütterich *et al.* [5]’s data to 74-like. We can see that the agreement between our ionization balance and Foster [8]’s is generally poor, but consistently so up to 10-like. This is because the contribution from DR is small compared to that of RR from 01-like ($\sim 99\%$). This contribution from DR gradually increases until it becomes comparable to RR at 10-like, and goes on to exceed this as the residual charge of the ion decreases. Another factor causing the difference is the application of the Jüttner relativistic correction to the DR/RR rate coefficients for our calculation, but not that of Foster’s.

10-like tungsten

As mentioned in the Introduction, DR of 10-like tungsten has been considered by Behar, Mandelbaum, and Schwob [17] and Safronova, Safronova, and Beiersdorfer [16]. In Figure 4 we compare the total DR rate coefficients calculated in this work with the data calculated by Behar *et al* and Safronova *et al* . It can be seen that our rate coefficients sit somewhere between the two. Typically, the difference between our rate coefficients and Behar *et al* ’s do not exceed 10% at peak abundance temperature, whereas the difference is typically $> 40\%$ when comparing to Safronova *et al* ’s data. These differences may arise due to the way the higher- n DR is calculated. In the case of Behar *et al* ’s and Safronova *et al* ’s data, radiative and Auger rates are calculated up to a nominal value of n (typically 8–15), which are then extrapolated up to $n \sim 1000$. This extrapolation method may miss additional Auger channels opening-up at higher- n , whereas our method described previously allows for their inclusion in the calculation. In the future, it will be prudent to assess the sensitivity of the extrapolation method to the final explicit n calculated before extrapolation is used.

Future work and conclusions

To date, we have completed calculations for 01-like to 37-like. Calculations are currently ongoing for 38-like – 57-like. All data that will be generated will be hosted on the OPEN-ADAS website¹ in the standard *adf09* and *adf48* formats. In these proceedings we have introduced *The Tungsten Project*, and have described its aims, and the data that will be produced. We have used AUTOSTRUCTURE to calculate partial DR/RR rate coefficient data for ionization stages 01-like – 37-like tungsten. One paper has been published covering 01-like – 18-like, and we are currently writing a second paper for 19-like – 36-like. We are currently conducting calculations covering the *4d* and *4f* shells, and expect these to be completed in a timely fashion. We are aiming to calculate updated CR models incorporating the new data described here.

¹<https://www.open.adas.ac.uk>

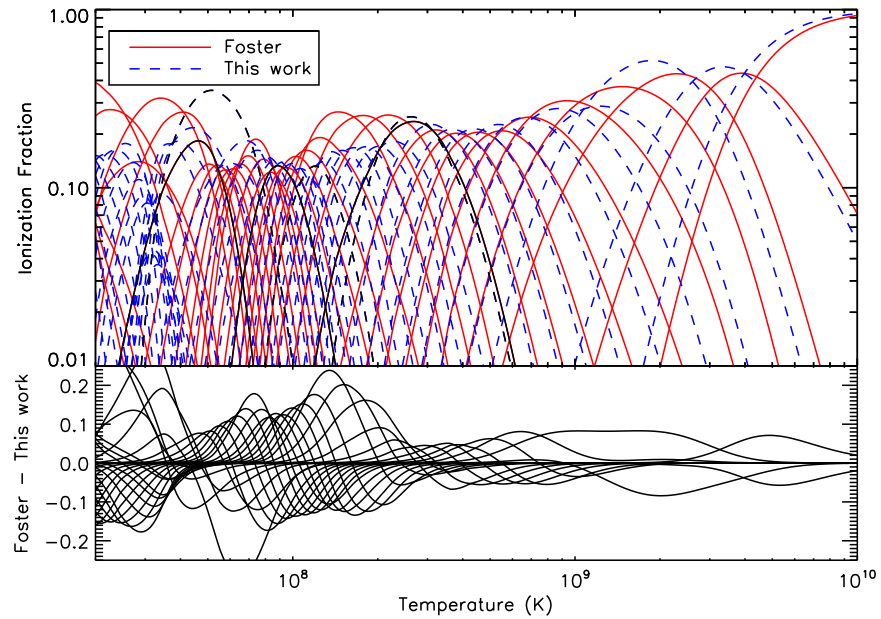


FIGURE 3. Comparison of ionization balances using recombination data calculated in this work (blue dashed curve), and that of Foster [8] (red solid curve) up to 18-like tungsten. Again, both curves use ionization rate coefficients from Loch *et al.* [10]. The black lines indicate (from right to left) the positions of 10-like and 18-like tungsten.

ACKNOWLEDGMENTS

This work was supported by the Engineering and Physical Sciences Research Council (EPSRC), Grant No. EP/1021803 to the University of Strathclyde.

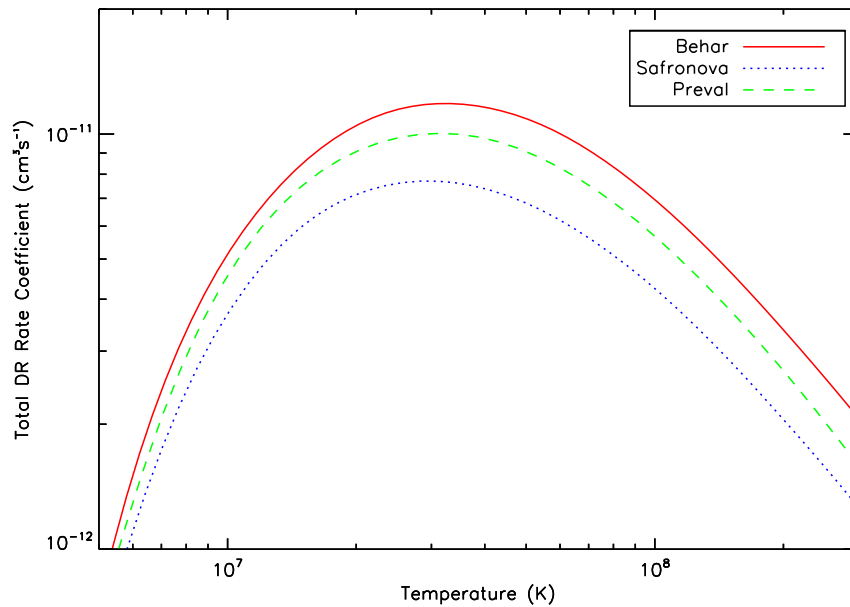


FIGURE 4. Comparison of total DR rate coefficients for 10-like tungsten calculated by Behar, Mandelbaum, and Schwob [17] (red solid line), Safronova, Safronova, and Beiersdorfer [16] (blue dashed line) and in this work (green dotted line).

REFERENCES

- [1] G. F. Matthews, M. Beurskens, S. Brezinsek, M. Groth, E. Joffrin, A. Loving, M. Kear, M. L. Mayoral, R. Neu, P. Prior, V. Riccardo, F. Rimini, M. Rubel, G. Sips, E. Villedieu, P. de Vries, M. L. Watkins, and E.-J. Contributors, *Physica Scripta* **2011**, 014001 (2011).
- [2] F. Romanelli and J. E. F. D. A. Contributors, *Nuclear Fusion* **53**, 104002 (2013).
- [3] H. K. Chung, M. H. Chen, W. L. Morgan, Y. Ralchenko, and R. W. Lee, *High Energy Density Physics* **1**, 3 (2005).
- [4] L. B. Zhao and S. C. Li, *Phys. Rev. A* **55**, 1039 (1997).
- [5] T. Pütterich, R. Neu, R. Dux, A. D. Whiteford, M. G. O’Mullane, and the ASDEX Upgrade Team, *Plasma Physics and Controlled Fusion* **50**, 085016 (2008).
- [6] D. E. Post, R. V. Jensen, C. B. Tarter, W. H. Grasberger, and W. A. Lokke, *Atomic Data and Nuclear Data Tables* **20**, 397 (1977).
- [7] D. Post, J. Abdallah, R. E. H. Clark, and N. Putvinskaya, *Physics of Plasmas* **2**, 2328 (1995).
- [8] A. R. Foster, “On the Behaviour and Radiating Properties of Heavy Elements in Fusion Plasmas,” Ph.D. thesis, University of Strathclyde, http://www.adas.ac.uk/theses/foster_thesis.pdf 2008.
- [9] A. Burgess, *ApJ* **141**, 1588 (1965).
- [10] S. D. Loch, J. A. Ludlow, M. S. Pindzola, A. D. Whiteford, and D. C. Griffin, *Phys. Rev. A* **72**, 052716 (2005).
- [11] Z. Wu, Y. Fu, X. Ma, M. Li, L. Xie, J. Jiang, and C. Dong, *Atoms* **3**, 474 (2015).
- [12] M. F. Gu, *ApJ* **590**, 1131 (2003).
- [13] D. H. Kwon and W. Lee, *JQSRT* **170**, 182 (2016).
- [14] A. Bar-Shalom, M. Klapisch, and J. Oreg, *Journal of Quantitative Spectroscopy and Radiative Transfer* **71**, 169 (2001).
- [15] A. Peleg, E. Behar, P. Mandelbaum, and J. L. Schwob, *Phys. Rev. A* **57**, 3493 (1998).
- [16] U. I. Safronova, A. S. Safronova, and P. Beiersdorfer, *Atomic Data and Nuclear Data Tables* **95**, 751 (2009).
- [17] E. Behar, P. Mandelbaum, and J. L. Schwob, *Phys. Rev. A* **59**, 2787 (1999).
- [18] S. P. Preval, N. R. Badnell, and M. G. O’Mullane, *Phys. Rev. A* **93**, 042703 (2016).
- [19] N. R. Badnell, *Journal of Physics B: Atomic and Molecular Physics* **19**, 3827 (1986).

- [20] N. R. Badnell, *Journal of Physics B: Atomic, Molecular and Optical Physics* **30**, 1 (1997).
- [21] N. R. Badnell, *Computer Physics Communications* **182**, 1528 (2011).
- [22] D. W. Savin, E. Behar, S. M. Kahn, G. Gwinner, A. A. Saghir, M. Schmitt, M. Grieser, R. Repnow, D. Schwalm, A. Wolf, T. Bartsch, A. Müller, S. Schippers, N. R. Badnell, M. H. Chen, and T. W. Gorczyca, *ApJS* **138**, 337–370 (2002).
- [23] N. R. Badnell and M. S. Pindzola, *Phys. Rev. A* **39**, 1685 (1989).